INT. J. REMOTE SENSING, 1987, VOL. 8, NO. 7, 981–996

Spatial and temporal behaviour of a large agricultural area as observed from airborne C-band scatterometer and thermal infrared radiometer

J. V. SOARES,† R. BERNARD and D. VIDAL-MADJAR

Centre de Recherches en Physique de l'Environnement,
38/40 rue du Général Leclerc, 92131 Issy-les-Moulineaux, France

(Received 19 December 1986; in final form 9 March 1987)

Abstract. Natural thermal emission in the 8–12 μm band as well as emission or diffusion of microwaves at low frequencies are known to be strongly correlated with the soil surface water content. Theoretical studies of the interaction between the soil/plant system and the atmosphere have shown that such measurements may be used to monitor the soil water budget. Experimental results from an airborne campaign are presented here. The surface temperature and radar cross-section spatial properties and their interrelations are examined for very different situations (wet and dry, bare and vegetated). It is shown that, as far as large-scale applications are concerned, the field scale can be considered as homogeneous for both measurements and that it is possible to derive meaningful regional information from measurements at that scale. Therefore, at least for the test region, a high spatial resolution (of microwaves and thermal infrared measurements) is not required for the monitoring of surface soil moisture and thermal equilibrium for this 10-day period.

1. Introduction

For bare land, the soil water content is known to be a determining factor in the variation of such quantities as land albedo, surface temperature or microwave emissivity (see, for example, Schmugge *et al.* 1980). The soil skin temperature (T_s) is governed by the energy budget at the soil/atmosphere interface. It is then a function of the atmospheric forcing (available energy) and of the thermal properties of the soil. These properties depend on the soil type and on its water content. For instance, the variation of T_s together with a good knowledge of the atmospheric forcing can be used to estimate the bare soil surface moisture (Carlson 1985).

The soil emissivity or reflectivity in the low-frequency microwave range is a function of a number of parameters including the surface roughness, the soil temperature and its dielectric properties. Due to the high value of the water dielectric constant, the wet soil permittivity is quite sensitive to the variation of the water content. In the case of active microwave measurements (scatterometer) the signal depends on the dielectric constant through the Fresnel reflection coefficient and then depends strongly on the surface water content (Ulaby *et al.* 1978).

In the case of a bare land surface then, both the thermal infrared and C-band radar cross-sections are sensitive to surface soil moisture. It is then of interest to look at the correlations between both measurements over an agricultural region and their relations with the land features. This paper presents such a comparison using the ERASME airborne equipment. It includes a C-band scatterometer which is fully described elsewhere (Bernard *et al.* 1986 b) and a Barnes PRT-5 radiometer to obtain

† Present address: Universidade Estadual Paulista, Departamento de Agricultura, 15378 Ilha Solteura-SP, Brasil.

the surface thermal signal. The scatterometer was optimized for a soil moisture mission (small incidence angle and HH polarization). In the first part, the experiment is described including a presentation of the test region and of the measurement geometry. Then for a few fields (bare and vegetated), the statistical properties of the surface temperature (T_s) and backscattering cross-section (σ_0) are given together with some of their variations in time. Finally, the same exercise is carried out for the entire area (36 km^2). It will be shown that despite the large-small scale heterogeneities (which in fact make very difficult a day-to-day comparison on a pixel by pixel basis) the field scale can be considered as homogeneous regarding the radar cross-section and the thermal infrared signal. It is therefore not necessary to achieve a resolution better than the mean field size for the use of remote sensing data in regional hydrology and climatology.

2. Experiment description

2.1. *The test region*

The test region is an agricultural area situated in the south-west of Paris. The experiment has been conducted over a very flat area of 36 km^2. It is constituted of large fields with very few tree clusters or hamlets. In 1983 it was essentially covered with wheat and corn (80 per cent wheat and 20 per cent corn). A map of the area is shown in figure 1 where specific fields have been outlined (and labelled from 1 to 12). They correspond to fields where the airborne remote sensing data have been thoroughly examined. For the six bare fields, the soil granulometry is given in table 1. At the centre of the area was the central experimental site where field measurements were taken: atmospheric forcing (wind, air temperature, humidity and surface energy fluxes), soil water budget and surface soil moisture measurements (for radar calibration). Those measurements are partly described elsewhere (Bernard *et al.* 1986 a).

2.2. *The remote sensing equipment*

The ERASME remote sensing equipment is constituted of a C-band scatterometer and a thermal infrared radiometer. The radiometer is a commercial Barnes PRT-5 infrared thermometer and is mounted on the helicopter so that it looks in the same direction as the scatterometer antenna's axis.

The scatterometer is a C-band Frequency Modulated Continuous Wave radar which has been designed to study the active microwave signatures of natural surfaces. It is fully described elsewhere (Bernard *et al.* 1986b). Table 2 gives its main characteristics. For the present experiment it has been used in the optimal configuration for soil moisture campaigns (Ulaby *et al.* 1978), namely HH polarization and

Table 1. Granulometric analysis of the soils from the six bare fields shown in figure 1, expressed in parts per thousand.

Field	Clay	Fine silt	Coarse silt	Fine sand	Coarse sand
1	271	319	354	25	31
3	262	316	375	20	27
4	230	328	412	17	13
5	271	346	346	16	21
9	275	324	375	14	12
11	255	331	387	16	11

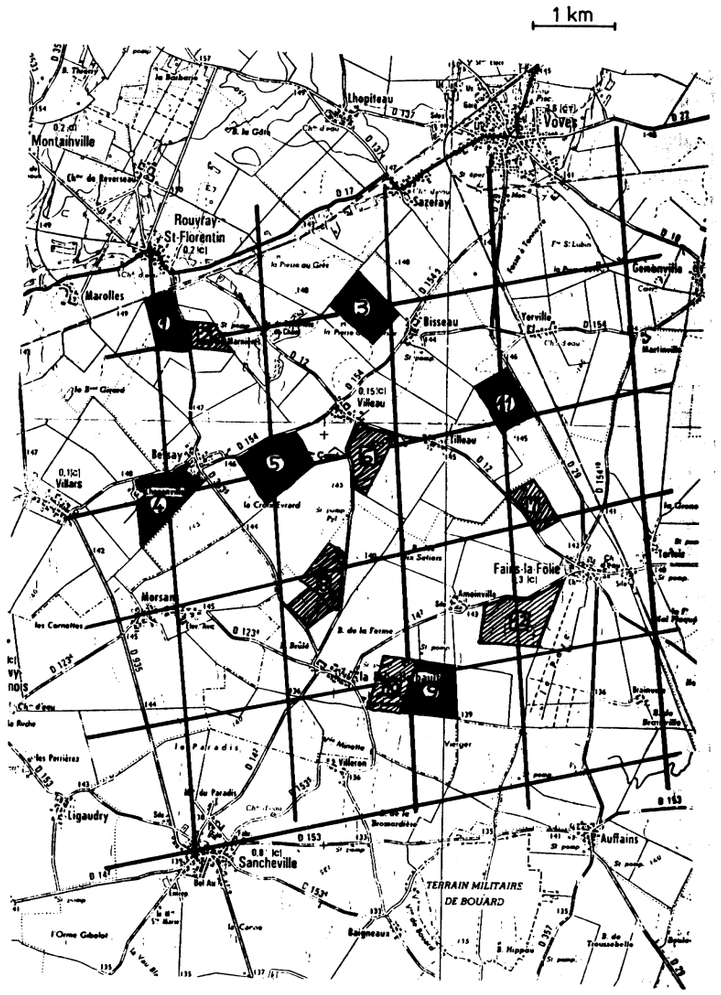

Figure 1. Map of the test area. It consists of a 6 × 6 km^2 region. The theoretical flight lines are represented together with the location of the 12 particular fields. The black ones were wheat covered and the shaded ones were corn covered.

antenna boresight at an incidence angle of 13°. The flying altitude was about 350 m. At that height the instantaneous field of view at 13° is 11 m along track and 12 m cross track. In order to minimize the speckle effects, the signal is integrated on board over 200 ms (64 samples). At the helicopter speed of 40 ms^{-1}, this corresponds to one point every 8 m which is very comparable with the along track theoretical resolution.

Table 2. ERASME radar characteristics.

Type	FM-CW
Frequency	5·35 GHz (C-band)
Transmitted power	15 mW (11·6 dbm)
Modulation	Triangular; period 6 ms
Bandwidth	220 MHz (adjustable)
Transmitting antenna	Corrugated horn; gain 18·3 dB; 3 dB beamwidth 12·6°
Receiving antenna	Planar dipoles array; gain 25·2 dB (VV), 23·2 dB (HH); beamwidth 2·3° × 5·6° (VV), 1·8° × 8·5° (HH)
Receiver gain	101·3 dB ± 0·4
Signal processing	FFT analyser; 512 pts.; 500 Hz resolution; synchronized with the modulation waveform; available bands 120–220 kHz, 150–250 kHz, 240–340 kHz; data recorded on CCT
Internal calibration	Bulk acoustic wave device delay 2 μs; attenuation 61·5 dB; coupler attenuation 30 dB
Ancillary data	Clock; flight parameters (pitch, roll, heading, pressure altimeter); eight analogue data lines

2.3. *Experimental procedure*

The experiment was held in two periods in 1983. The first one at the end of June and beginning of July corresponds to the mature state of the wheat and to the beginning of the corn growth. For the second one, in September, the wheat has been harvested since the end of July and some fields have already been ploughed. At that period, the corn is nearly mature (it is generally harvested during the month of October).

The ideal flight lines are drawn on the map (figure 1), being six north/south and six east/west transects. The flights were made over 9 days in July and 10 days in September at a time near local solar noon. The actual paths are estimated using an on-board video recording together with the images obtained with the radar where such features as tree stands, roads or hamlets are easily identified. The navigation errors correspond to the precision of the time recording which was 1 s (corresponding to about 40 m). But it may be smaller in the case of a sharp transition on the radar data between two fields.

The swath width of the calibrated radar image was about 135 m ranging from 25 m to 160 m from the vertical sub-helicopter point. For soil moisture application, the pixels corresponding to the 11° (± 1°) incidence angle are considered which correspond to a cross-track resolution of 12 m. The along-track resolution is given by the antenna aperture and may easily be checked on the radar image autocorrelation function (figure 9). Consequently each radar point for soil moisture application is representative of a $12 \times 12\,m^2$ field of view. The helicopter path could not be reproduced from one flight to another with that accuracy. Actually the flight path discrepancy can reach 100 m or more. The comparison of the data from one day to another is then complicated by small-scale heterogeneities of the surface backscattering properties.

2.4. *The scatterometer calibration for soil moisture*

Soil samples from 0 to 10 cm have been taken from seven fields located in the vicinity of the central site. Those fields were either bare or vegetation covered. For the entire campaign, 29 comparison points were obtained after exclusion of the cases where the helicopter did not fly over the ground plots. The relationship between the radar backscattering for an inclination angle of 11° ± 1° and the measured soil water content was calculated from these data. When w, water content in the first 10 cm, is

expressed in cm^3/cm^3 (which is the physical quantity which controls the σ_0 variation with the moisture content (Dobson *et al.* 1985)), the regression gives

$$w = 0{\cdot}30 + 0{\cdot}016\,\sigma_0(\text{dB}) \quad (1)$$

where σ_0 is the absolute backscattering coefficient averaged over all the fields.

Other calibration experiments were held in 1985 and 1986 on a small watershed (part of the Brie region, east of Paris). The calibration points obtained in 1983, 1985 and 1986 are plotted in figure 2. The regression gives

$$w = 0{\cdot}30 + 0{\cdot}015\,\sigma_0(\text{dB}) \quad (2)$$

with a correlation coefficient $R = 0{\cdot}89$ for 45 points.

3. Discussion of the measurements

The remote sensing measurements have been processed in order to examine a few important points. The surface soil moisture is known to be highly variable with a small spatial correlation length (Nielsen *et al.* 1973, Vauclin *et al.* 1983). One of the advantages of airborne or spaceborne remote sensing is to give access to large-scale measurements. It is then necessary to understand the meaning of the field average soil moisture or temperature. This involves the characterization of the variability of T_s (surface temperature) and σ_0 (backscattering coefficient) within the fields and how it varies in different situations (bare and vegetated, dry and wet). It will be shown that the observed mean relations between T_s and σ_0 are not in contradiction with the known behaviour of the soil/plant/atmosphere system and that they give important informations about the significant spatial scale for regional applications.

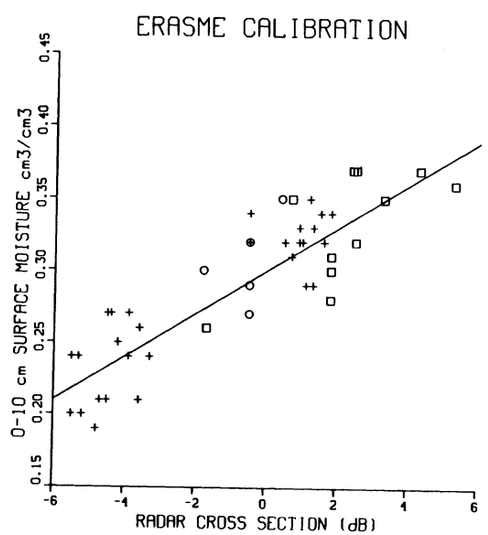

Figure 2. Correlation line between radar backscattering (σ_0) and volumetric water content (w). Crosses are for the 1983 experiment, circles for the 1985 experiment and squares for 1986.

3.1. *Example of radar signals from individual fields*

The variation of the radar signal within the field number 5 is plotted in figure 3 for three dates (20, 23 and 28 September). This field can be considered as reasonably homogeneous. It has been overflown both from south to north (path B) and from east to west (path A).

The drying of the field along that period is easily seen, with the average σ_0 decreasing from about 0 dB to -5 dB (which corresponds, using the calibration curve (2), to a decrease in surface soil moisture from 0·30 to 0·22 cm^3/cm^3). However, some structure within the field can be observed, especially on the first day, with the southwestern side of the field more humid than the northern part. This structure is still observed, but dampened, along the drying period on path B (south/north). The east/west plot (path A) shows more variability, and the comparison from one day to the other is not easy as the transect on the second day (23 September) has been flown about 50 m northward of the others. This variability within the field, which is related to intra-field heterogeneities, may reach 5 dB which is equivalent to 0·075 cm^3/cm^3.

This example shows that the comparison of spot ground truth with high resolution radar is not easy as it requires a good co-location of the spots. Another conclusion would be that only statistical properties of the σ_0 over a field are meaningful for comparison between fields, or for the same field at different times.

3.2. *Statistical properties within a field*

In figures 4 and 5 are plotted the histograms of T_s (measured by the PRT-5) and σ_0 (at 11° measured by the radar) for the bare field number 11 (table 1) for 3 days (20, 23 and 29 September). The behaviour of T_s and σ_0 are not identical. On 20 September, T_s and σ_0 exhibit little dispersion and thus the field can be considered as homogeneous. On 23 September, T_s is still homogeneous but σ_0 shows a bimodal distribution. This fact is easily explained, as this particular field was partly ploughed. The lowest mode corresponds to the stubble. All the fields of the test region ploughed between 20 and 23 September have a higher signal on the 23 September than the other parcels. It is a ploughing effect which mixes the drier soil of the surface with wet soil from deeper layers. This does not affect the surface temperature. At the end of the drying, on 29 September, the σ_0 is again perfectly unimodal, the field being fully ploughed, but the temperature exhibits a large heterogeneity. This particular feature may be due to the growing resistance to evaporation which depends greatly on the local thermal and hydraulic properties. In contrast, figures 6 and 7 show the same type of histogram but for the corn field number 6. Here the radar signal, and thus the surface soil moisture, appears to be reasonably homogeneous and only decreases slightly. This is not the case for the surface temperature which always exhibits a higher variability than for the bare soil.

Examination of figures 4, 5, 6 and 7 shows that, in most cases, it is possible to define meaningful means for T_s and σ_0 for a given field. For example, this has been done on σ_0 for the six bare fields listed in table 1. For each field a mean value of σ_0 is calculated. Figure 8 shows, as a function of time, the evolution of this mean value and its standard deviation. The response of the radar signal to rainfall is clearly visible. On the other hand if the same exercise is done for the corn fields (figure 8) such a response to rainfall is not found. This may be due partly to the corn canopy water interception and to a direct transfer of the water to a sub-surface layer due to the root system and to the stalks. Another feature is that the dispersion is almost constant except, in the bare soil cases, for 23 September which may be due partly to agricultural work and partly to a

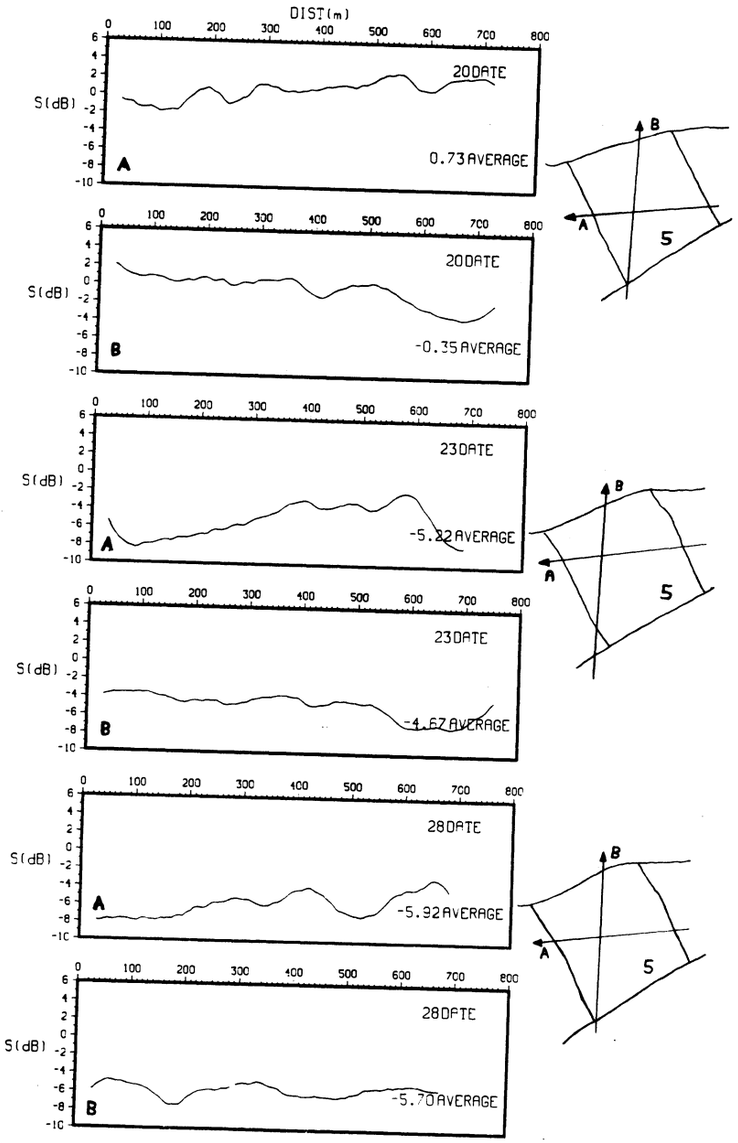

Figure 3. Evolution of the radar backscattering (σ_0) for the bare field number 5 (table 1). That field was flown once south/north (path B) and a second time east/west (path A). The precise paths are indicated for 20, 23 and 28 September. The signal heterogeneity is very sensitive to the location of the measurements.

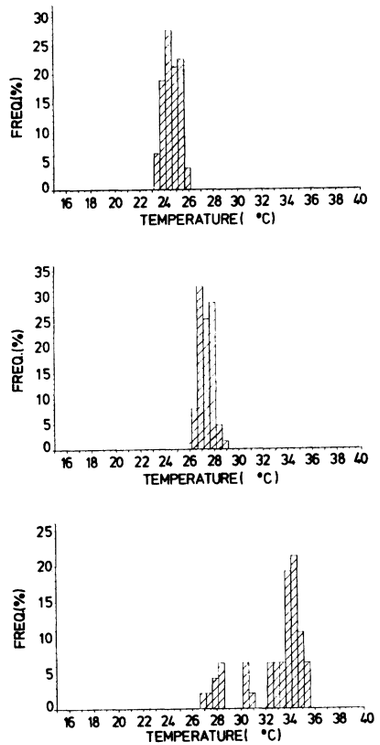

Figure 4. Histograms of the surface temperature (T_s) for the bare field number 11 for 3 days: 20 (wet), 23 (drying) and 29 September (dry). The field can be considered as homogeneous except for on 29 September which may be due to heterogeneities in surface thermal properties.

heterogeneity of the hydraulic properties of the soil surface layer (Bernard *et al.* 1986a). The dispersion is small enough not to hide the general evolution of the radar signal during the experiment.

3.3. *Relations between* T_s *and* σ_0 *over the entire site*

The surface temperature T_s can be used to estimate the resistance of the soil/plant system to evaporation or transpiration (Taconet *et al.* 1986). This resistance is strongly related to available water within the root zone for a vegetation-covered surface or within the surface layer in the case of bare soil. Important in understanding the physical mechanisms which link the surface temperature and the surface water content are their spatial correlation lengths. This is shown in figures 9 and 10. In figure 9, the autocorrelation function of T_s and σ_0 are plotted for 20 and 29 September. The

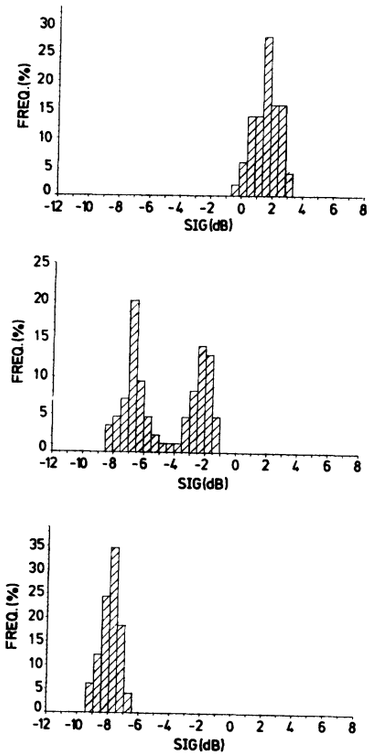

Figure 5. Same as for figure 4 but for radar backscattering. The heterogeneity on 23 September is due to a partial ploughing.

correlation lengths appear to be very similar. For comparison, the autocorrelation function obtained using series which represent the nature of the surface seen along the same transect (1 for bare soils, −1 for corns and 0 for hamlets and towns, called the 'background') is also shown. It exhibits the same correlation length (first null at approximately 400 m). In figure 10 are plotted more instructive functions, namely the cross-correlation between T_s and σ_0 or the background and between σ_0 and the background. It is clear that although the autocorrelation functions are similar they are not due to the same causes. T_s is always well correlated with the background which shows that the governing parameter is the nature of the canopy (difference between corn and bare soils). On the other hand, if σ_0 is correlated with the background on the dry day (see below for discussion), it is not the case on the wet day. It shows that the correlation length of σ_0 for the 20 September is not due to the background. It may be a consequence of soil drainage heterogeneities as discussed in Bernard *et al.* (1986a).

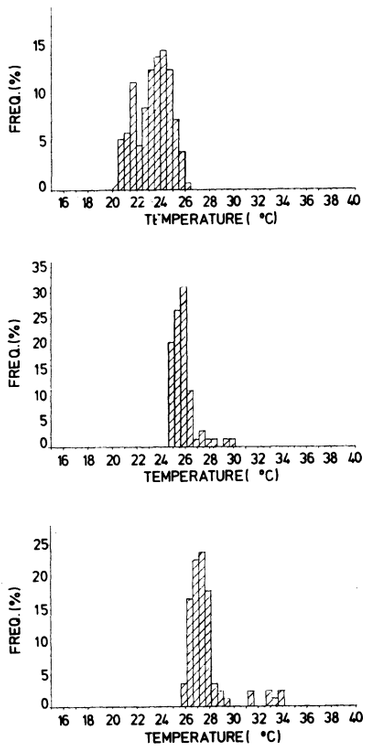

Figure 6. Same as for figure 4 but for corn field number 6.

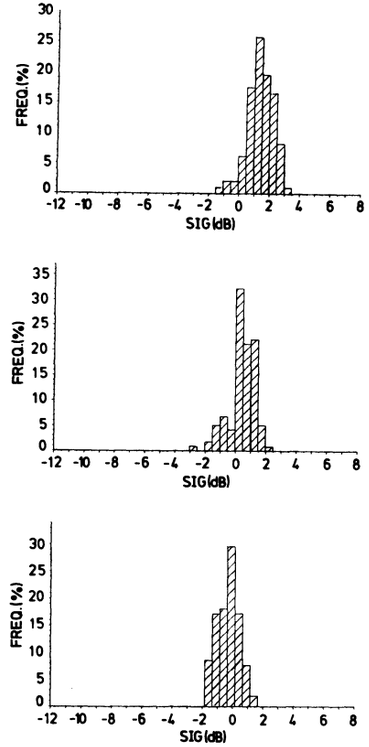

Figure 7. Same as for figure 5 but for corn field number 6.

Thus it can be seen that the field scale can be considered as homogeneous and that it is not necessary when dealing with regional problems to have a resolution of better than 400 m, at least for this type of region.

Another way to look at the difference between bare and vegetated soils is to consider their signatures in a T_s/σ_0 diagram. Figure 11 is an illustration of this. It represents a two-dimensional histogram (T_s and σ_0) of all the data for the wet day (20 September) and the dry day (29 September).

On the wet day there is no correlation between the two variables. This is due to the fact that after the preceding rainfalls, the water in the corn root zone or in the bare soil surface layer is sufficient to provide the evaporation required by the atmospheric demand. On the other hand for the dry day it is possible to distinguish two populations. The first has roughly the same σ_0 as 20 September but a higher temperature and corresponds to the corn data. The other has a very low σ_0 and a very high temperature and corresponds to the bare field. The σ_0 (and therefore the surface water content) is higher in the case of the corn, due to the shelter effect of the canopy which hinders the Sun from heating the soil surface and then hinders evaporation. In that case there is still no correlation between σ_0 and T_s which confirms the fact that the soil surface water content is not a governing parameter for the transpiration. In the case of bare soil, a correlation between σ_0 and T_s is clearly visible (the coefficient of linear correlation is equal to 0·58). Here, the dryer the soil surface, the higher the resistance to evaporation and thus the surface temperature. The relatively poor correlation may be explained by the fact that the radar signal is sensitive to the first 5 or 10 cm of soil water content whereas the resistance to evaporation is in fact related to the water of a more shallow layer which will certainly be dryer.

4. Conclusion

An analysis of an airborne remote sensing campaign has been presented. Its originality lay in the combination of active microwave and passive thermal infrared

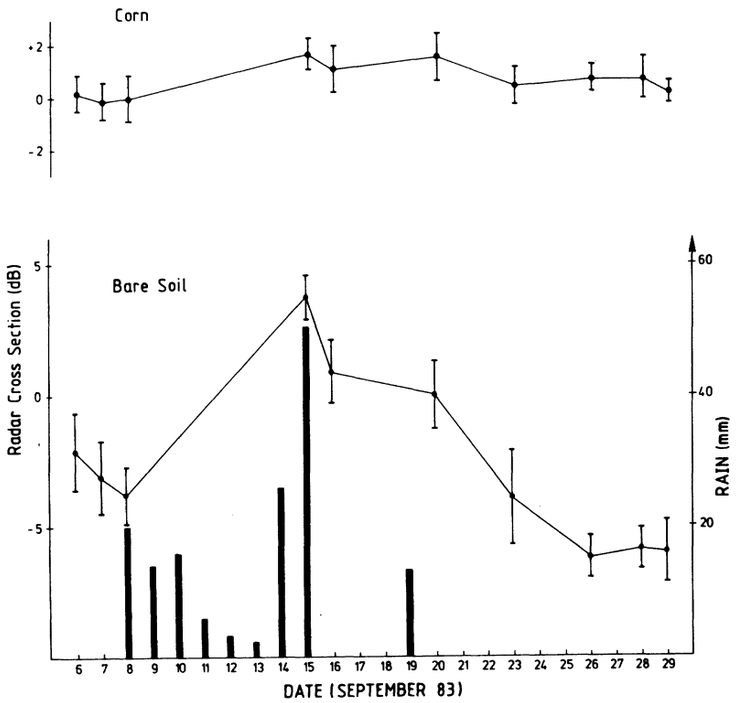

Figure 8. Evolution during September 1983 of the mean backscattering coefficient over the six bare fields and the six corn fields (figure 1) and the standard deviations. The rainfall rates for each day are plotted in mm of water per day. The very different responses to rainfall and to drying are the most striking feature.

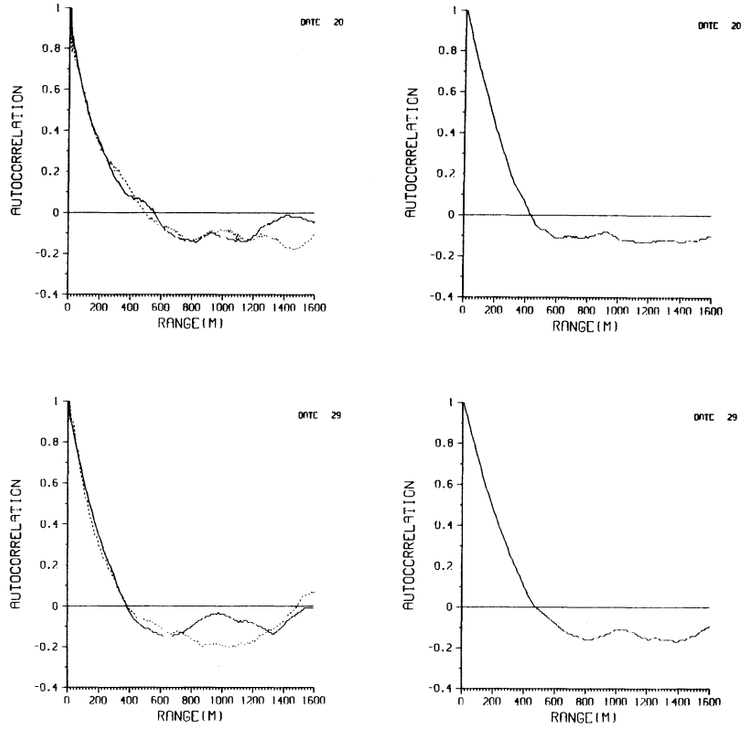

Figure 9. Autocorrelation functions of σ_0 and T_s (σ_0 solid line, T_s dashed line) and of the background (right) for 20 (top) and 29 (bottom) September. The correlation lengths for T_s and σ_0 are comparable with that of the background (first null at roughly 400 m). The correlation length does not depend on the hydraulic state of the surface (wet for the 20, dry for the 29 September).

remote sensing which are both sensitive to soil water content. The large number of flights over the test region in 1 month has given access to the fields' signatures for various situations (bare and corn fields, dry and wet). Several results have been found from the statistical study of the acquired data. They have several consequences either in the definition of the water content at field scale or in a system design for soil surface water content monitoring. It has been shown that the field scale (either bare or covered by vegetation) can be considered as a meaningful entity in regard to surface temperature and surface moisture (as deduced from radar measurement). It has been shown also that the spatial behaviour of T_s is always correlated with the fields canopy which is not the case for σ_0. The spatial heterogeneities of σ_0 are not only due to vegetation but may be due to other soil parameters such as drainage capability, especially on the wet days. Consequently, if it is admitted that the radar signal is a reliable measurement of surface soil moisture, microwave remote sensing gives an easy access to such an important quantity as the surface water content at field scale. Furthermore, it has also been shown that the response of the radar signal for this 10-day period, for this particular region shows sufficient spatial homogeneity to avoid the necessity of dealing with high-resolution radar images. It is anticipated that a resolution of about 0·05 km^2 may be sufficient as far as it is possible to discriminate between essentially bare or vegetated areas. This is the first experimental confirmation of the simulation results obtained some years ago by Dobson *et al.* (1982).

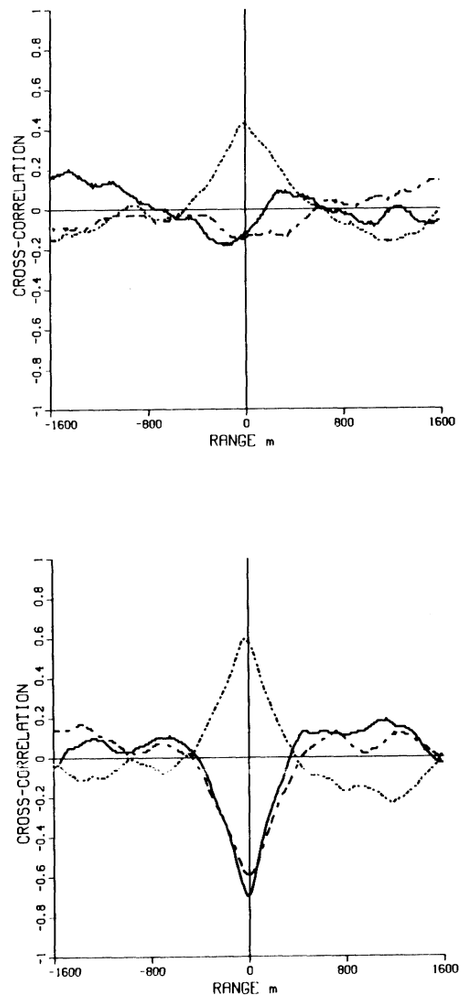

Figure 10. Cross-correlation of T_s versus σ_0 (solid), T_s versus background (dotted) and σ_0 versus background (dashed) for the 20 (top) and 29 (bottom) September. T_s is always well correlated with the background. This is not the case for σ_0 on the wet day (20 September). The correlation length of σ_0 on 20 September is not due to the mean field size.

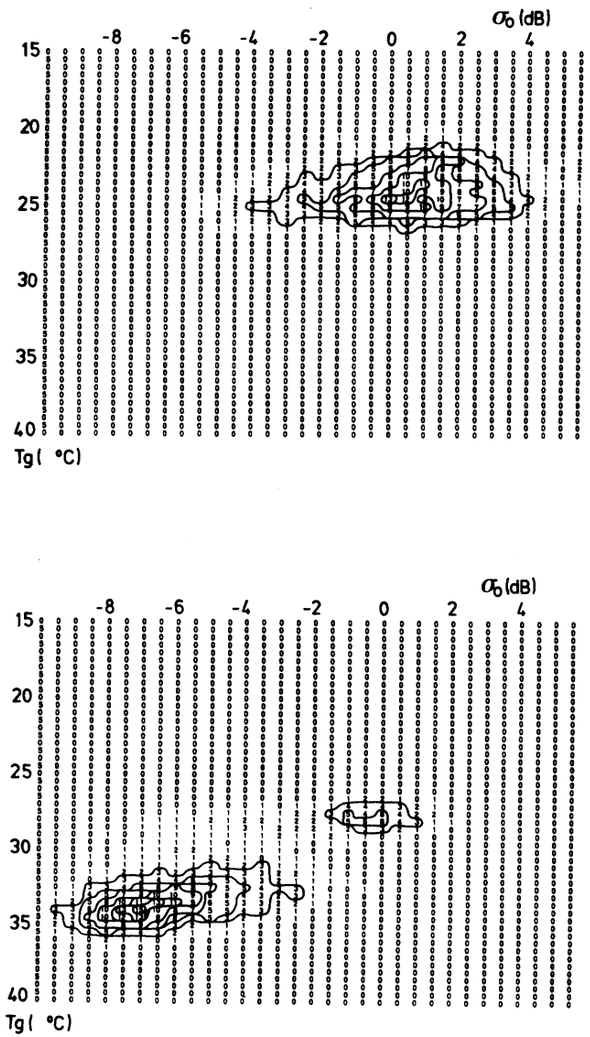

Figure 11. Bi-dimensional histograms between T_s (labelled T_g) and σ_0 for 20 (top) and 29 (bottom) September. The bare and vegetated points are clearly separated on 29 September.

Acknowledgments

The ERASME radar has been built by the CRPE with CNES funding and support. This research has been supported by the Centre National d'Etudes Spatiales, the Centre National de la Recherche Scientifique and the Centre National d'Etudes des Télécommunications. J. V. Soares was supported by the Brazilian FAPESP.

References

BERNARD, R., SOARES, J. V., and VIDAL-MADJAR, D., 1986a, Differential bare fields drainage properties from airborne microwave observations. *Wat. Resour. Res.*, **22,** 869–875.

BERNARD, R., VIDAL-MADJAR, D., BAUDIN, F., and LAURENT, G., 1986b, Data processing and calibration for an airborne scatterometer. *I.E.E.E. Trans. Geosci. remote Sensing*, **24,** 709–716.

CARLSON, T. N., 1985, Regional scale estimates of surface moisture availability and thermal inertia using remote thermal measurements. *Remote Sensing Rev.*, **1,** 197–247.

DOBSON, M. C., ULABY, F. T., HALLIKAINEN, M. T., and RAYES, E. L., 1985, Microwave dielectric behavior of wet soil. Part II: dielectric mixing models. *I.E.E.E. Geosci. remote Sensing*, **23,** 35–46.

DOBSON, M. C., ULABY, F. T., and MOEZZI, S., 1982, Assessment of radar resolution requirements for soil moisture estimation from simulated satellite imagery. Remote Sensing Laboratory Technical Report 551-2, University of Kansas Center for Research, Lawrence, Kansas.

NIELSEN, D. R., BIGGAR, J. W., and ERHT, K. T., 1973, Spatial variability of field measured soil water properties. *Hilgardia*, **42,** 215–259.

SCHMUGGE, T. J., JACKSON, T. J., and MCKIM, H. L., 1980, Survey of methods for soil moisture determination. *Wat. Resour. Res.*, **16,** 961–970.

TACONET, O., BERNARD, R., and VIDAL-MADJAR, D., 1986, Evapotranspiration over an agricultural region using a surface flux/temperature model based on NOAA/AVHRR data. *J. Climate appl. Met.*, **25,** 284–307.

ULABY, F. T., BATLIVALA, P. P., and DOBSON, M. C., 1978, Microwave backscatter dependence on surface roughness, soil moisture and soil texture. Part I, Bare soil. *I.E.E.E. Trans. Geosci. remote Sensing*, **16,** 286–295.

VAUCLIN, M., VIERA, S. R., BERNARD, R., and HATFIELD, J. T., 1983, Spatial variability of surface temperature along two transects of a bare soil. *Wat. Resour. Res.*, **18,** 1677–1686.